# SUPPLEMENTAL INFORMATION

## Inventory of Supplemental Information

### SUPPLEMENTAL FIGURES AND LEGENDS

**Figure S1**, related to Figure 1: Observed correlations in cell fates are consistent with an early random commitment and geometrical constraints at later stages.

**Figure S2**, related to Figure 2: Marker expression in maternal zygotic Gata6 mutant, wild-type and heterozygote embryos at different stages and in outgrowths.

**Figure S3**, related to Figure 3: CDX2 expression in ICM cells after prolonged culture in FGF.

**Figure S4**, related to Figure 5: NANOG/GATA6 negative cells in the ICM of FGF-treated embryos are OCT4 positive.

### SUPPLEMENTAL TABLES

**Table S1**, related to Figure 2: Genotypes of embryos recovered from *Gata6* heterozygous intercrosses at various stages.

### SUPPLEMENTAL MOVIES

**Video S1**, related to Figure 3: *Pdgfra*$^{H2B\text{-}GFP}$ PrE reporter is not activated during *Gata6* mutant blastocyst development.

### SUPPLEMENTAL EXPERIMENTAL PROCEDURES

## SUPPLEMENTAL FIGURES AND LEGENDS

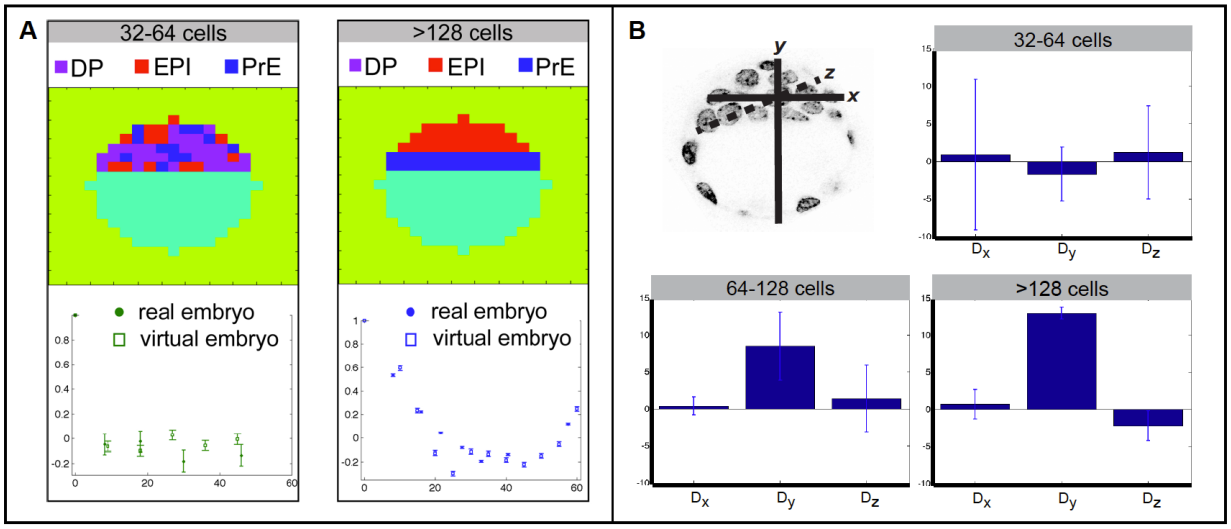


**Figure S1, related to Figure 1: Observed correlations in cell fates are consistent with an early random commitment and geometrical constraints at later stages.**

**A** simplified 2D geometry mimicking the mouse blastocyst was generated on a uniformly spaced lattice. Cell fates were assigned either randomly (32-64 cell stage) or in a pattern resembling the embryo after sorting of PrE and EPI cells. The Pearson's correlation coefficient of cell fates as a function of cell distance was computed for virtual embryos and compared to the measured data of real embryos. The simulated dependency of the correlation function is in good agreement with the measured correlations, suggesting that early cell fate specification is controlled by random commitment, and that the correlations observed in late embryos are controlled by their geometry. **B** Average difference in the (x,y,z) coordinates of EPI and PrE cells as a function of developmental stage (see cartoon for information on coordinates; at the 32-64 cells stage, this computation was performed on the few cells that have already committed to EPI or PrE fate- see data in Figure 1B). At all stages, embryos do not show asymmetries in x and z, as expected. At the 32-64 cells stage, there is no asymmetry in y, suggesting that early commitment is controlled by cell autonomous stochastic factors. Asymmetries in y become evident at the 64-128 cells stage and further increase at the >128 cells stage. These observations suggest that the movement of EPI cells away from the cavity and PrE cells towards the cavity is subsequent to the random cell fate commitment observed at the earlier stages.

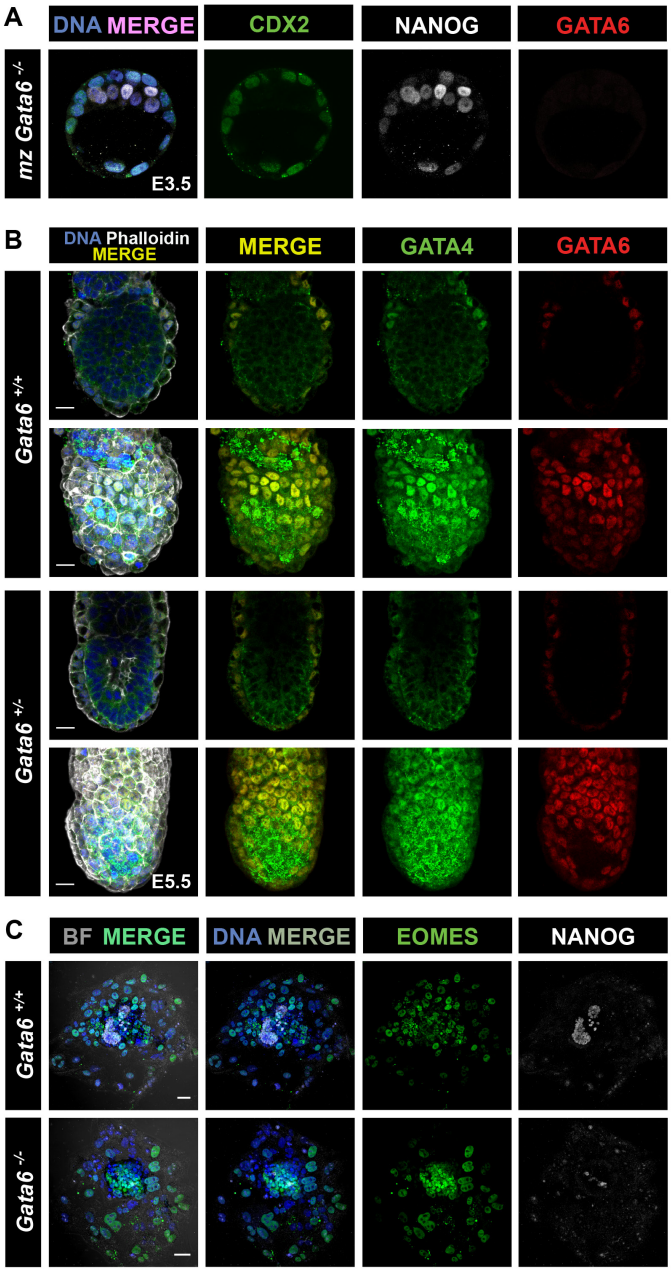


**Figure S2, related to Figure 2: Marker expression in maternal zygotic Gata6 mutant, wild-type and heterozygote embryos at different stages and in outgrowths.**

**A** Localization and distribution of CDX2 (green), NANOG (white) and GATA6 (red) in maternal zygotic E3.5 *Gata6* mutant blastocysts. Blue in merge: Hoechst. **B** Localization and distribution of GATA4 (green) and GATA6 (red) in E5.5 *Gata6*$^{+/+}$ and *Gata6*$^{+/-}$ embryos. Blue in merge: Hoechst. White in merge: Phalloidin. C Localization and distribution of EOMES (green) and NANOG (white) in outgrowths of *Gata6*$^{+/+}$ and *Gata6*$^{-/-}$ embryos 4 days after plating. Blue in merge: Hoechst. BF: Brightfield.

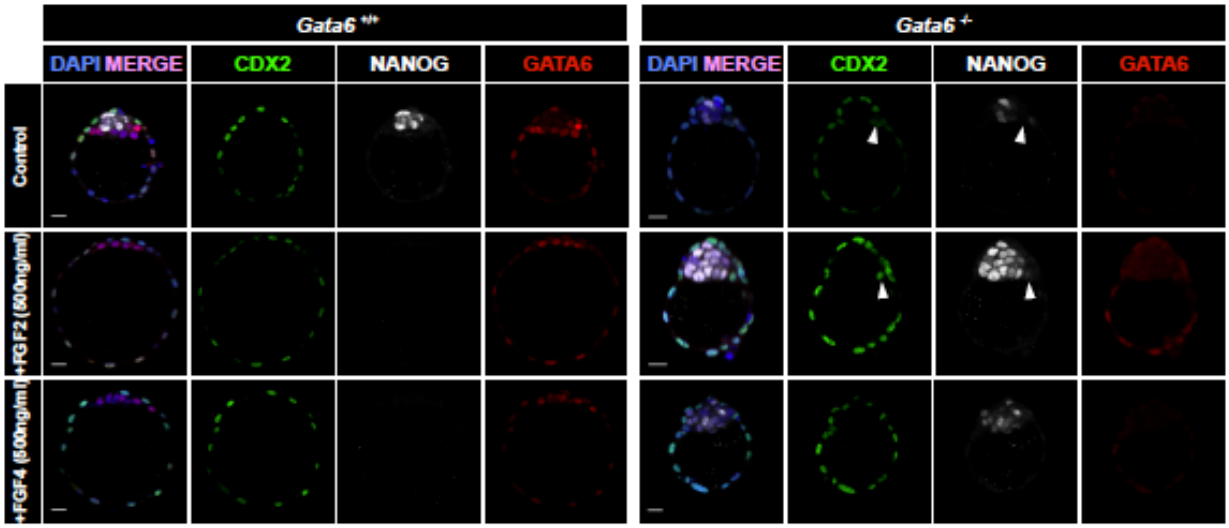


**Figure S3, related to Figure 3: CDX2 expression in ICM cells after prolonged culture in FGF**.

Localization and distribution of CDX2 (green), NANOG (white) and GATA6 (red) in *Gata6* wild-type and mutant mouse embryos. Embryos were cultured from the 8-cell stage (E2.5) for 72h to assess whether the population of CDX2+ cells in the ICM expanded over time as a consequence of exposure to FGF. Arrowheads indicate CDX2 expressing cells in the ICM.

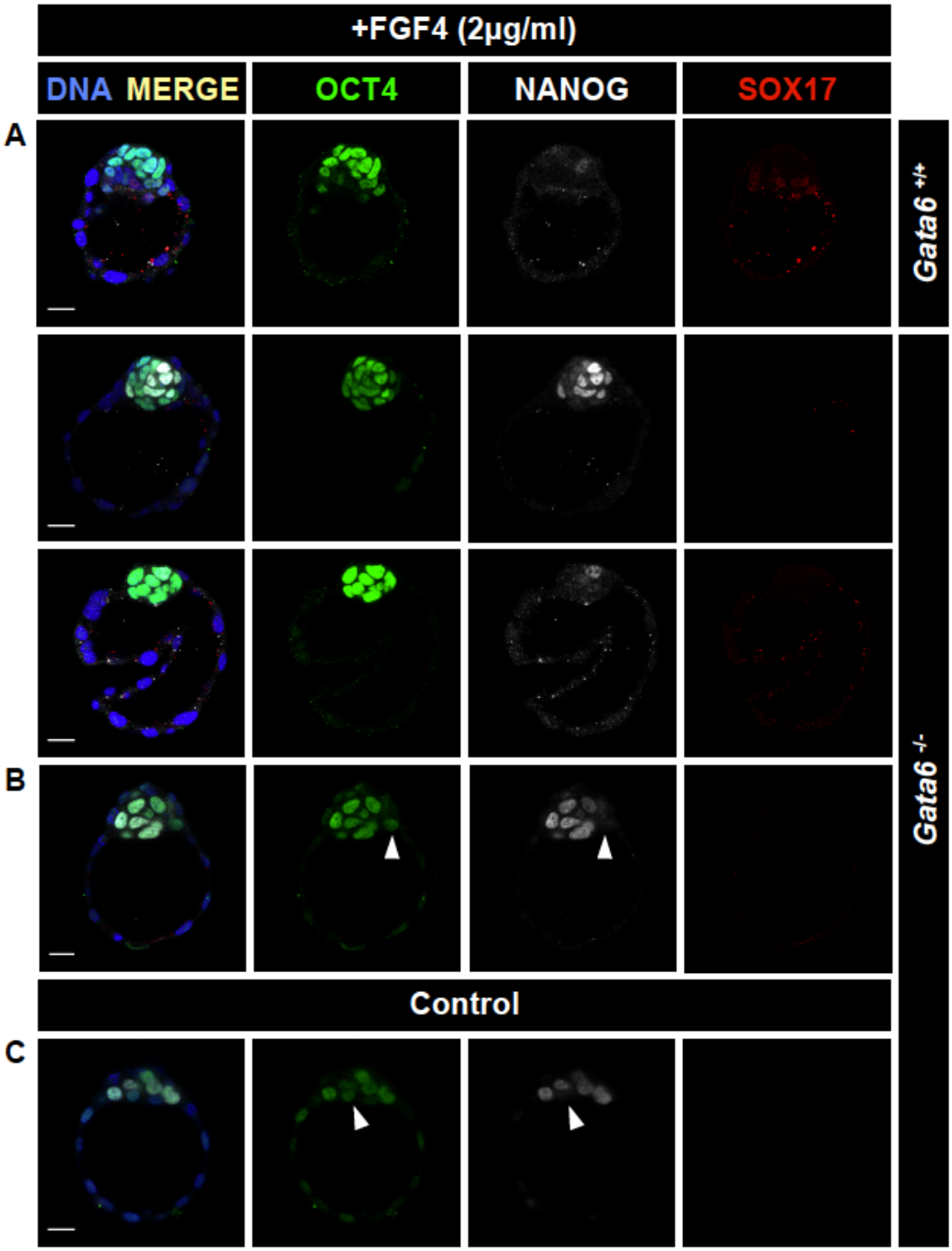


**Figure S4, related to Figure 5: NANOG/GATA6 negative cells in the ICM of FGF-treated embryos are OCT4 positive.**

Localization and distribution of OCT4 (green), NANOG (white) and SOX17 (red) in *Gata6* wild-type and mutant blastocysts after culture in 2 µg/mL FGF from E3.5 for 24 h **(A)**, from E2.5 for 48 h **(B)** and untreated **(C)**. Blue in merge: Hoechst.

## SUPPLEMENTAL TABLES

| | Genotype | | | |
|---|---|---|---|---|
| **Stage of embryo** | ***Gata6*$^{+/+}$** | ***Gata6*$^{+/-}$** | ***Gata6*$^{-/-}$** | **Total no. of embryos recovered** |
| <64 cells **early blastocyst** | 28 | 68 | 34 | 130 |
| 64-128 cells **mid-blastocyst** | 19 | 40 | 20 | 79 |
| >128 cells **late blastocyst** | 10 | 10 | 12 | 32 |
| E5.5 **post-implantation** | 8 | 34 | 0 | 42 |

**Table S1, related to Figure 2: Genotypes of embryos recovered from *Gata6* heterozygous intercrosses at various stages.**

## SUPPLEMENTAL MOVIES

**Video S1, related to Figure 3: *Pdgfra*$^{H2B\text{-}GFP}$ PrE reporter is not activated during *Gata6* mutant blastocyst development.**

(see accompanying movie file)

Time series of early to late blastocyst stage embryos from a *Gata6*$^{+/-}$; *Pdgfra*$^{H2BGFP}$ x *Gata6*$^{+/-}$ cross. Time-total: 20 h; time interval: 15 min; z-total: 62 µm; z-interval: 2 µm. Labels indicate genotypes.

## SUPPLEMENTAL EXPERIMENTAL PROCEDURES

### Image data acquisition and processing

Laser scanning confocal images of immunostained embryos were acquired on a Zeiss LSM 510 META. Embryos were mounted in PBS on glass-bottom dishes. Fluorescence was excited with a 405-nm laser diode (Hoechst), a 488-nm Argon laser (GFP, Alexa Fluor 488), a 543-nm HeNe laser (Alexa Fluor 543, 555) and a 633-nm HeNe laser (Alexa Fluor 633 and 647). Images were acquired using a Plan-Neofluar 40×/1.3 Oil DIC objective, with an optical section thickness of 1–1.2 µm. Raw data were processed using ZEN (Carl Zeiss Microsystems), ImageJ (NIH) and MINS (Lou et al., 2014) software. 3D time-lapse imaging was performed on a Zeiss LSM 510 META. Embryos were placed in drops of KSOM under mineral oil on glass-bottom dishes (MatTek Corp). Time intervals between z-stacks were 15 minutes, for 15-20 hours total. Raw data were processed using Zeiss ZEN software (Carl Zeiss Microsystems).

### Image segmentation and quantitative fluorescence intensity analysis pipeline

For cell counting and quantification MINS software (http://katlab-tools.org/) was used (Lou et al., 2014). Confocal images in *.lsm format were loaded into the MINS pipeline, which detects nuclei, accurately segments them and exports results of nuclear count, size, position and fluorescence intensity of all channels in table format, and as images of numbered nuclei (Figure 1). The MINS output was checked for over- or under-segmentation and tables were corrected manually. Mitotic cells were also found and excluded from the analysis. TE cells were defined molecularly and positionally, as nuclei positive for CDX2 in cells located on the surface of the embryo. For representation of fluorescence intensity distribution throughout ICMs, data was subject to logarithm transformation to reduce the technical variability due to the loss of fluorescence along the z-axis. For statistical comparison of intensity distributions, these values were plotted as the average log intensity per embryo rather than per cell. A Wilcoxon Mann-Whitney Test was performed to compare two populations, a Kruskal-Wallis Test for more than two populations. All analysis of fluorescence intensity levels and statistics were performed using R (http://www.r-project.org/). For correlation and probability functions nuclear concentrations were extracted from nuclear intensity measurements by first subtracting background fluorescence, and then correcting for the decrease in fluorescence intensities due to tissue depth in z-stacks of image data. Background intensities for both NANOG and GATA6

were estimated from the average fluorescence intensity values (at the >128 cell stage) of half of the TE cells having the lowest intensities. The value obtained for GATA6 was comparable to the one obtained by imaging *Gata6*$^{-/-}$ embryos and the value for NANOG was very low and similar to the one observed in PrE cells at late stages, thereby validating our procedure. A correction factor as a function of axial position (z coordinate) in the embryo was estimated by determining how the signal intensity of the DAPI channel scaled with z. The DAPI intensities of all nuclei in an embryo were fitted as a function of z using the Smoothing Splines function in MATLAB (http://www.mathworks.com/products/matlab/), and the fit was then used to correct the fluorescence intensities. The number of PrE and EPI cells was established using the threshold functions shown in Figure 1B. Correlation functions were computed by evaluating the Pearson's correlation coefficient for each pair of cells as a function of the distance between them. The probabilities of cell specification (as well as their 95% confidence intervals) as a function of cell number were estimated through logistic regression using the Curve Fitting Toolbox in MATLAB.

**Genotyping**

Following image acquisition embryos were genotyped as described previously (Kang et al., 2013a) using the following primers: Gata6cKO fw: 5′-GTGGTTGTAAGGCGGTTTGT-3′, Gata6cKOrev: 5′-ACGCGAGCTCCAGAAAAAGT-3′, Gata6KOfw: 5′-AGTCTCCCTGTCATTCTTCCTGCTC-3′, Gata6KOrev: 5′-TGATCAAACCTGGGTCTACACTCCTA-3′, GFPfw: 5′-AAGTTCATCTGCACCACCG-3′, GFP rev: 5′-TGCTCAGGTAGTGGTTGTCG-3′.

**Embryo-derived stem cell derivation and culture**

ES cell lines were derived from embryos collected from Gata6+/– intercrosses according to standard procedures (Czechanski et al., 2014). Embryonic day (E) 3.5 embryos were on mitotically inactivated murine embryonic fibroblast (MEF) feeder cells for 9 days. Outgrowths were disaggregated and passaged into 24-well dishes. Medium was replaced every 2 days. Emerging ES cell colonies were passaged into new 24-well plates until confluence. Cells were then cultured in the absence of MEFs and genotyped. All cells were grown at 37°C in 5% CO2. ES cells were routinely cultured as described previously (Kang et al., 2013a).

**RT-PCR**

RNA from *Gata6*$^{+/+}$ and *Gata6*$^{-/-}$ ES cells was isolated using Trizol Reagent (Life Technologies) according to the manufacturer's instructions. Reverse transcription (RT) and genomic DNA digestion was performed using QuantiTect Reverse Transcrption Kit (Qiagen) according to the manufacturer's instructions. PCR was performed on the prepared cDNA using the following primer sequences: *Gapdh*-fw: 5'-GTGTTCCTACCCCCAATGTGT-3', *Gapdh*-rev: 5'-ATTGTCATACCAGGAAATGAGCTT-3', *Gata6*-fw: 5'-AGACGGCACCGGTCATTACC-3', *Gata6*-rev: 5'-TCACCCTCAGCATTTCTACGCC-3', *Nanog*-fw: 5'-TGCGGACTGTGTTCTCTCAGG-3', *Nanog*-rev: 5'-CCACTGGTTTTTCTGCCACCG-3', *Fgf4*-fw: 5'-ACTACCTGCTGGGCCTCAAA-3', *Fgf4*-rev: 5'-AAGGCACACCGAAGAGCTTG-3', *Fgfr1*-fw: 5'-CACCTGCATCGTGGAGAATG-3', *Fgfr1*-rev: 5'-CAAGTTGTCTGGCCCGATCT-3', *Fgfr2*-fw: 5'-CCTTCGGGGTGTTAATGTGG-3', *Fgfr2*-rev: 5'-GGGTACAGCATGCCAGCAAT-3'. Primers were designed for amplicons to span exon borders to avoid possible amplification of genomic DNA. *Gata6* primers were designed to bind outside of Exon2, which is deleted in *Gata6* mutant cells.

Supplemental Figure 1

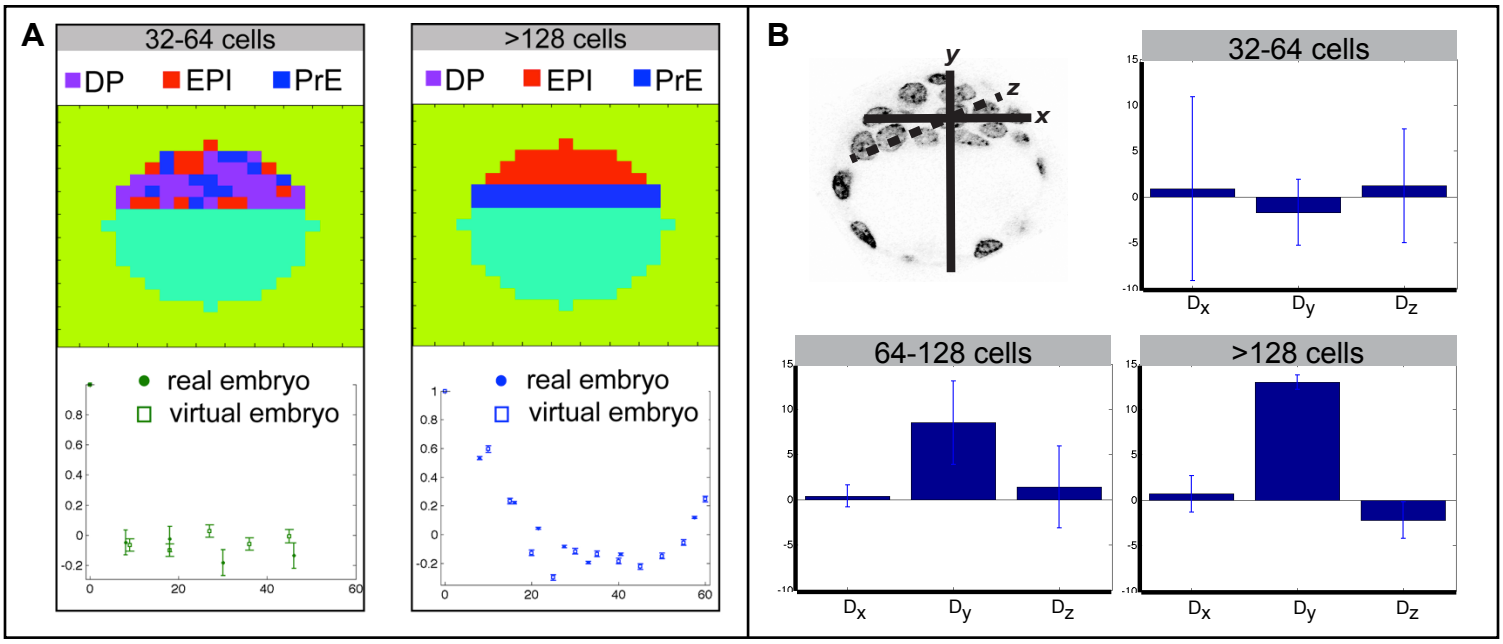


Schrode et al., Figure S1, related to Figure 1

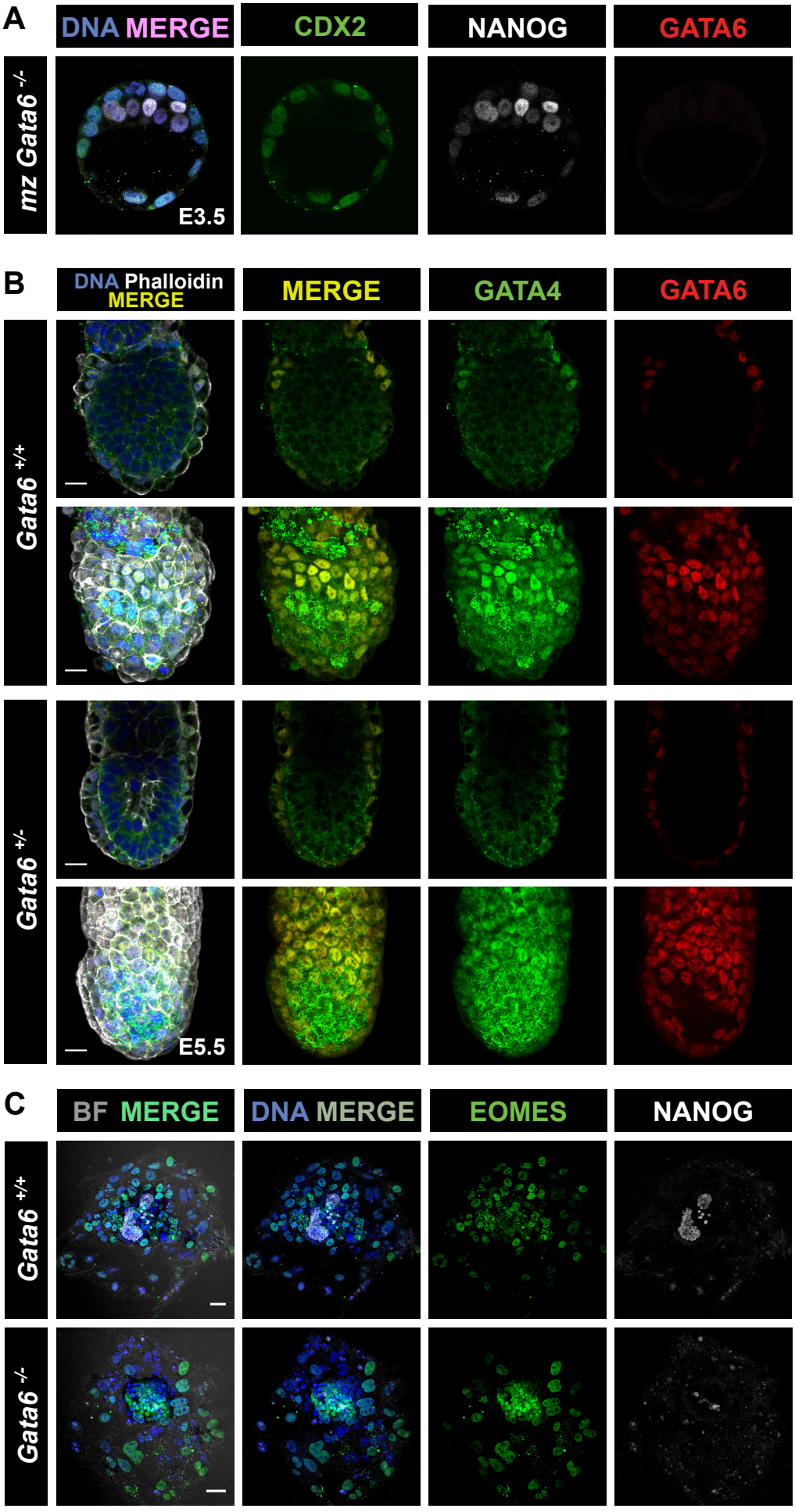


Schrode et al., Figure S2, related to Figure 2

Supplemental Figure 3

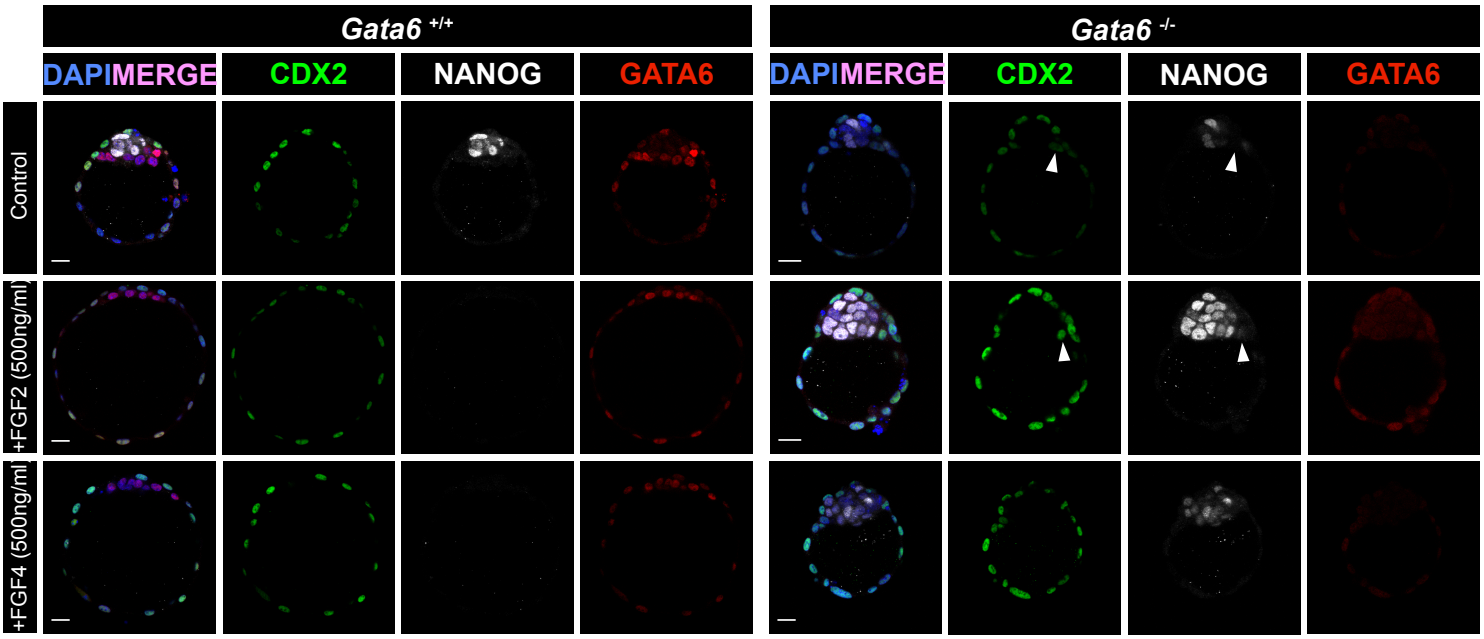


Schrode et al., Figure S3, related to Figure 3

Supplemental Figure 4

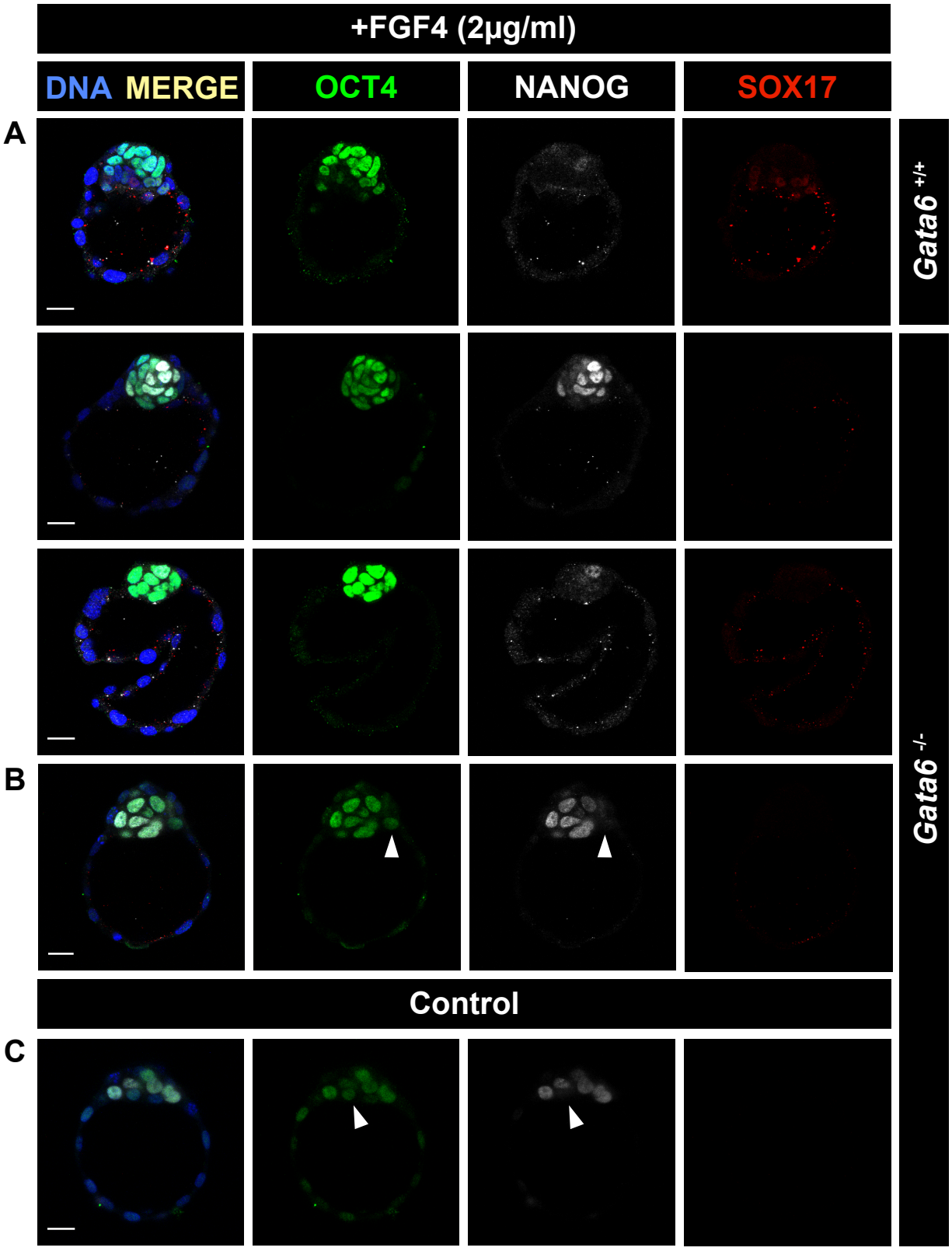


Schrode et al., Figure S4, related to Figure 5